Desalination and Water Treatment
www.deswater.com

doi: 10.5004/dwt.2021.27311

228 (2021) 242–252
July

Effect of MgO and montmorillonite nanoparticles on removal behavior of cobalt

Soheil Seif[a,*], Safar Marofi[a], Shahriar Mahdavi[b]

[a]*Water Engineering Department, Faculty of Agriculture, Bu-Ali Sina University, Hamedan 6517833131, Iran, Tel. +98 81 34224528/+98 9370555282; Fax: +98 81 34224012; emails: soheilseif65@gmail.com (S. Seif), smarofi@yahoo.com (S. Marofi)*
[b]*Department of Soil Science, Faculty of Agriculture, Malayer University, Malayer, Iran, Tel. +98 9188110848; email: smahdaviha@yahoo.com*

Received 3 September 2020; Accepted 9 April 2021

ABSTRACT

In this research, the adsorption of divalent cobalt (Co(II)) ions from aqueous solutions were investigated using nano magnesium oxide (MgO-NPs) and montmorillonite nanoparticles (Mont-NPs). Batch experiments were carried out to measure the optimum values of pH, adsorbent dosage, contact time, and temperature. Adsorbents were characterized by powder X-ray diffraction and a scanning electron microscope with energy-dispersive X-ray. Thermodynamic parameters were calculated, and the results showed an exothermic and endothermic pattern for the adsorbents. The maximum adsorption capacities of MgO-NPs and Mont-NPs were calculated as 440 and 2.53 mg/g, respectively. The pseudo-second-order model justified the experimental data of the adsorbents, while the pseudo-first-order model only fitted the MgO-NPs data. Desorption was carried out at the last point of the isotherm figure to verify the preservation capability of the adsorbed ions. Regarding the adsorbent dosage and the isotherm experiments, this study revealed that MgO-NPs have an excellent potency for Co(II) ion adsorption from the aqueous solutions compared to Mont-NPs. MgO-NPs and Mont-NPs are present in some rocks and soil textures; hence, the finding of this study could help chemists and environmentalists with the trace of pollutants and the removal of heavy metals in the soil-water medium.

Keywords: Adsorption; Isotherms; MgO; Montmorillonite; Nanoparticles; Co(II) ion

1. Introduction

During recent decades, environmental contamination has been one of the most eye-catching issues, which have attracted worldwide attention owing to an increase in heavy metal ions in water, air, and soil media. Nowadays, pollution of biological resources and water bodies by heavy metal ions is one of the biggest problems, threatening human society [1]. Heavy metal ions can enter into the food chain of humans and organisms; thus, removing heavy metals is a promising way to make the environment a better place to live. The expansion of the industry and the increasing population of the planet have all resulted in a growing demand for worldwide water consumption. Simultaneously, increased municipal and industrial waste in the environment and lack of drinkable water escalated the pollution in water and soil, particularly in the industrial cities, which is alarming for the present and future generations.

Cobalt (Co) is a heavy metal known to cause toxicities at high concentrations. It is a trace element that occurs naturally and is widely distributed via mining, metallurgical productions and nuclear plants across the globe [2]. Cobalt is an essential element of cellular metabolism; moreover, it is proven that cobalt is a constituent of vitamin B_{12}, which is involved in adjusting blood pressure and has a significant impact on thyroid functioning [3]. Nevertheless, exposure to

* Corresponding author.

high dosages of cobalt may result in health problems (such as neurotoxicological disorders and genotoxicity) and cancer [4]. Toxicity and harmful effects of excessive amounts of cobalt upon humans and organisms make it necessary to remove it from water and wastewater, mainly before entering the environmental cycle. Numerous techniques, such as co-precipitation, ion exchange, precipitation, reverse osmosis, oxidation and adsorption have been used to remove Co from water [2].

Among the various mentioned methods of heavy metal ions removal from contaminated water, the adsorption method has been favored because of its high efficiency, simplicity, adsorbent variability, and lower cost compared to the other approaches [5]. Many researchers believe that metal oxides have higher adsorption efficiency; individually, nano magnesium oxide (MgO-NPs) demonstrated a high capacity in the adsorption of ions [6–8]. Besides, MgO-NPs have minimal impact on the environment, and it has low solubility in water. MgO-NPs because of their high surface area, high alkalinity, and high PZC; meanwhile, minimum harmful effects on the environment can be used to treat polluted water [9,10]. The effect of MgO and $Mg(OH)_2$ has been assessed in studies related to toxic ions and pollution removal from water [11]; namely, Campbell and Starr [12] proven that metal ions (Cu, Ag, and Pb) can combine with MgO-NPs by the covalent bond. Pioneering investigations on MgO-NPs inspired us to conduct more studies about this powerful adsorbent by considering the effect of changing parameters and its efficiency rates.

Clays can be categorized as hydrated aluminosilicates, which are well known as the minerals that make up the colloid fraction (<2 μm) of soils, sediments, pebbles, and water [13]. Montmorillonite, as a type of clay, has a 2:1 layer structure in which an octahedral sheet is between two tetrahedral silica sheets [14]. Metal ions and water molecules can be placed into its layer structure, which would lead to the adsorption of heavy metal ions in the solution. Montmorillonite has a high ion exchange capability and specific surface, which enables it to absorb heavy metals from aqueous solutions; the negative surface charge of this material contributes to the retention of cationic ions [15]. Montmorillonite particles can remove cationic metal ions from solutions by electrostatic and ion exchange phenomena. On the other hand, by dint of their negative surface charge, they repel negative ions, which could be solved by modification techniques [16].

In this work, MgO-NPs and montmorillonite nanoparticles (Mont-NPs) were considered for Co(II) ion adsorption, and to reach the optimum condition of the removal process, the following parameters were measured. The effects of pH, adsorbent dosage, temperature, and adsorption contact time were investigated; besides, the adsorbents characterizations were analyzed by powder X-ray diffraction (XRD) and scanning electron microscope with energy-dispersive X-ray (SEM-EDX) techniques.

2. Materials and methods

MgO-NPs (99% purity) and Mont-NPs (99% purity) were purchased from Nabond Technologies Co., Ltd., China Company. Synthesized $Co(NO_3)_2{\cdot}6H_2O$ was used to pollute deionized water. Co(II)-containing stock solution was prepared using $Co(NO_3)_2{\cdot}6H_2O$ to achieve the final concentration of 1,000 mg/L. Then it was diluted to various concentrations before use without pH adjustment. The concentrations of cobalt ions were determined using atomic absorption spectrometry analysis (Varian SpectrAA 220, Australia). HCl, HNO_3, and NaOH were purchased from Merck Co., Germany; all reagents were of analytical grade and used without purification. In all experiments, deionized water was used to be polluted. The pH of the solutions was measured by a pH meter (WTW Multi 3420), Germany. Characterization of the adsorbents was examined by the SEM-EDX (Philips XL30), Philips, The Netherlands; and XRD (XMD300) Unisantis, Germany, using Cu Kα radioactive source (λ = 0.154 nm) at 40 kV/40 mA. The size of the adsorbent particles was quantified by the Scherrer [Eq. (1)] as follows:

$$d = \frac{0.9\lambda}{b\cos\theta} \tag{1}$$

where λ is the wavelength of the X-ray (1.5418 Å), b is the XRD peak width at half-height, θ is the angle between the emitted ray and the sample, and d is the crystal size (nm), [17].

2.1. Preparing the solutions

Solutions were prepared by adding $Co(NO_3)_2{\cdot}6H_2O$ to deionized water; firstly, 1,000 ppm Co(II) solution was prepared, and then it was diluted to reach a specific concentration for each part of the research. The pH of the solutions was adjusted by adding NaOH (0.1 M) or HNO_3 (0.1 M).

2.2. Heavy metal adsorption analysis

All experiments were carried out in falcon tubes (50 mL) by adding 25 mL of solutions containing different Co(II) ion concentrations. The samples were shaken (90 rpm) to provide good contact between adsorbent and adsorptive (pollutant). For the isotherm experiment, the optimum used dosages of MgO-NPs and Mont-NPs were 0.05 and 5 g/L. In the case of pH, temperature, and adsorbent dosages experiment, their used dosages were 0.1 and 1 g/L, respectively. Co(II) concentrations were prepared up to 70 mg/L, and then they were diluted to reach the appropriate metal ions concentrations. Then, after shaking, the solutions were centrifuged (5,000 rpm) for 5 min to separate the solution from its solid part. At the last step, the supernatant liquid concentration was measured by using the atomic absorption spectrophotometer. The amount of adsorbed Co(II) concentrations was quantified by the following equation:

$$\text{Removal percentage} = \left(\frac{C_0 - C}{C_0}\right) \times 100 \tag{2}$$

where C_0 and C are the initial and final concentrations of Co(II) ions, respectively.

2.3. Effect of pH

pH has a determining impact on the adsorption process as it regulates the surface charge of the adsorbents and ionization. The effect of pH ranging (2–6) was measured, at the same time other conditions remained constant: (i) for Mont-NPs, Co(II) concentration was 7 mg/L, Mont-NPs dosage was 1 g/L, the room temperature was 25°C, and contact time was 240 min; (ii) MgO-NPs, Co(II) concentration was 70 mg/L, MgO-NPs dosage was 0.1 g/L, the room temperature was 25°C and contact time was 240 min. It is important to note that the pH above 6 was not considered in the process since the precipitation had occurred substantially at higher pH values.

2.4. Effect of adsorbent dosage

Adsorbent dosage experiment was conducted with MgO-NPs (0.05, 0.1, 0.2, 0.3. 0.4 and 0.5 g/L) and Mont-NPs (1, 2, 3, 4 and 5 g/L) dosages, Co(II) ion concentration of 70 mg/L, pH of solution, contact time of 240 min and room temperature at 25°C.

2.5. Effect of temperature

The solution was incubated at different temperatures, that is, 15°C, 20°C, 25°C, 30°C, and 35°C for 4 h to monitor the impact of temperature on heavy metal removal from the aqueous medium while other parameters remained constant.

2.6. Thermodynamic investigation

Thermodynamic parameters $\Delta G°$ (kJ/mol), $\Delta S°$ (J/mol K), $\Delta H°$ (kJ/mol) were measured by using the following equations [18], $\Delta G°$ measured by Eq. (4); also, $\Delta S°$ and $\Delta H°$ were measured by the slope and intercept of the linear regression of $\Delta G°$ vs. T by Eq. (5). The relevant equations are presented as follows:

$$K_c = \frac{q_c}{C_e} \tag{3}$$

$$\Delta G° = -RT \ln K_c \tag{4}$$

$$\Delta G° = \Delta H° - T\Delta S° \tag{5}$$

where K_c is the distribution coefficient of the adsorbate (dimensionless), q_c is the concentration of solid phase at equilibrium, C_e is the equilibrium concentration of metals in the solution (mg/L), T is the absolute temperature (K), and R (gas constant) which was 8.314×10^{-3} kJ/K/mol.

2.7. Effect of contact time

The effect of interaction time between adsorbents and Co(II) ions was investigated at five-time points (2, 10, 30, 60, and 240 min), while other parameters remained stable. As noted, Mont-NPs and MgO-NPs dosages were 1 and 0.1 g/L, respectively.

2.8. Kinetics modeling study

Pseudo-first-order model [Eq. (6)] [19], and pseudo-second-order model [Eq. (7)] [20], were implemented using the adsorption data, and the theoretical formulas are as given:

$$\log\left(q_e - q_t\right) = \log q_e - \left[\frac{K_1}{2.303}\right] t \tag{6}$$

$$\frac{t}{q_t} = \frac{1}{k_2 \cdot q_e^2} + \frac{1}{q_e} t \tag{7}$$

where q_e and q_t are the amounts of the adsorbates (mg/g) at equilibrium condition and at the time t (min), respectively. k_1 and k_2 are the constant values of the first (min^{-1}) and the second (g/mg min) order kinetic models, respectively.

The straight-line plot of $\log(q_e - q_t)$ against t was used to calculate the constant rate (k_1) for the pseudo-first-order model; furthermore, by linear regression of t/q_t against t, k_2 was determined.

2.9. Adsorption isotherm

Adsorption isotherm was conducted in different Co(II) ion concentrations (14, 28, 42, 56, and 70 mg/L). The solution pH, temperature, and contact time were regulated according to the optimum measured values. MgO-NPs and Mont-NPs dosages were 0.05 and 5 g/L, respectively. An isotherm equation usually represents the adsorption equilibrium, and its relevant parameters outline the favorable or unfavorable sorption process and absorbency of the adsorbent at a specific temperature and pH. It also gives information about the capacity of adsorbents; more specifically, the maximum mass of the adsorbate that an adsorbent can hold on its particles. Freundlich [Eq. (8)] and Langmuir [Eq. (9)] equations, [21] which commonly determine adsorption isotherm, are as follows:

$$\log q_e = \log K_f + \frac{1}{n} \log C_e \tag{8}$$

$$\frac{C_e}{q_e} = \frac{1}{q_{\max} . K_L} + \frac{C_e}{q_{\max}} \tag{9}$$

where q_e is the equilibrium solid phase (adsorbed metal ions on the adsorbent surface concentration) (mg/g), C_e is the equilibrium liquid phase concentration of the solution (mg/L), K_f is the Freundlich constant that signifies the adsorption capacity (mg/g), n is a dimensionless constant-coefficient which demonstrates the adsorption intensity, $q_{\max}$ is maximum adsorption capacity (mg/g), and K_L is equilibrium constant (L/mg).

2.10. Desorption experiments

In a solution, the exposure of adsorbed cations with anions may establish a chemical bond. These anions may break the bond between the adsorbent and the adsorptive. Accordingly, the effect of anions on adsorbed Co(II) ions was

examined by adding $CaCl_2$ to verify the Cl^- ion role in the process as well as the ability of the adsorbents for the retention of the adsorbate ions. As noted, the metal ions concentrations were 70 mg/L, and MgO-NPs and Mont-NPs dosages were 1 g/L and 5 g/L, respectively. After adsorption, 30 mL of deionized water was added to the batch residue, which was then shaken (1 h) and centrifuged (5 min, 5,000 rpm). Then, 30 mL of ethanol was added to the solid phase, and centrifuging was done (5 min, 5,000 rpm) to remove the liquid portion from its sediment. After that, 30 mL of $CaCl_2$ (0.01 M) was added to the sediment, which was shaken (1 h) twice in 24 h. Lastly, the samples were centrifuged (5 min, 5,000 rpm), and then the concentrations of Co(II) ion were determined by atomic absorption spectrometer.

To reach reliable data, all above experiments were repeated twice.

3. Results and discussion

3.1. Characterization of the adsorbents

SEM-EDX technique showed MgO-NPs have a nanoscale rod-shaped structure, which assists the adsorbent with having more contact surface for the adsorption of the ions. Moreover, it depicts this substance is porous and could entrap the ions. Fig. 1 indicates that Mont-NPs have a layer structure that empowers the adsorption process; besides, the nanostructure of montmorillonite facilitates the bonding between competitive elements.

EDX is an analytical technique widely used for the elemental analysis or characterization of a sample in chemistry. It was reported that MgO-NPs in this study have high purity, while Mg and O are the dominant elements of this material. Besides, the constituent ions of Mont-NPs are O, Si, Al, and Fe ions. There are many peak points in the XRD plot of the adsorbents, which show the crystalline structure of the materials. Mont-NPs, after adding to the deionized water, showed aggregation and swelling properties, which derive from the electrostatic surface charge of the particles and the percolation of water molecules through the layers. Accumulation of the particles is a barrier for the adsorption as it reduces the active surface sites.

The XRD plot determines the size of particles, which is available in Fig. 2. According to the Scherrer formula [Eq. (1)], the mean particle sizes of MgO-NPs and Mont-NPs were 26.1 and 28.4 nm, respectively. XRD patterns of MgO-NPs and Mont-NPs were identified by an X-ray diffractometer in the region 2θ of 10° to 90° at 25°C (Cu Ka, k51.54 Å). From Fig. 3, values are in good accordance with the literature report about MgO-NPs and Mont-NPs [8,22].

3.2. Effect of the initial pH

pH has a remarkable impact on the chemical reaction; notably, this could be more functional when heavy metal ions are near to a substance that can establish the covalent bonds or being full of functional groups. The pH point of zero charge (pH_{pzc}) is a concept in the adsorption process, which refers to the electric surface charge of the adsorbents [23]. The pH_{pzc} of Mont-NPs and MgO-NPs are 5.2 and 11.5, respectively [7]. Above the mentioned figures, the surfaces are negatively charged and lower than the cited figures; protons can be revealed [10,24]. The removal mechanism for MgO-NPs by laboratory observation was attributed to the adsorption and precipitation for pH < 5, and its primary agent for pH > 5 was precipitation and ion exchange, Fig. 4. $Co(OH)_2$ was a product of the reaction, and another output of the reaction could be $Co(OH)^+$ [25,26].

Because of the high exchangeable capability of clay particles, the Mont-NPs adsorption equilibrium rate was achieved by the adsorption and ion exchange mechanism. The presence of positive and negative ions, which influences

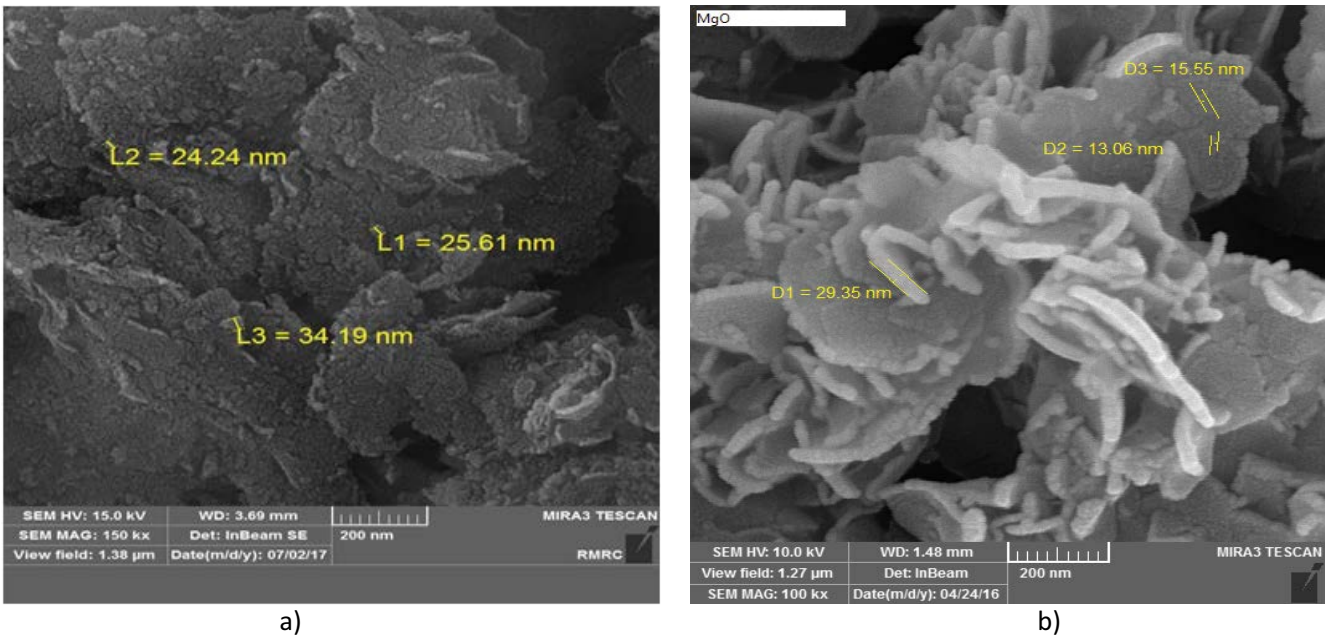

a) b)

Fig. 1. SEM images of Mont-NPs (a) and MgO-NPs (b).

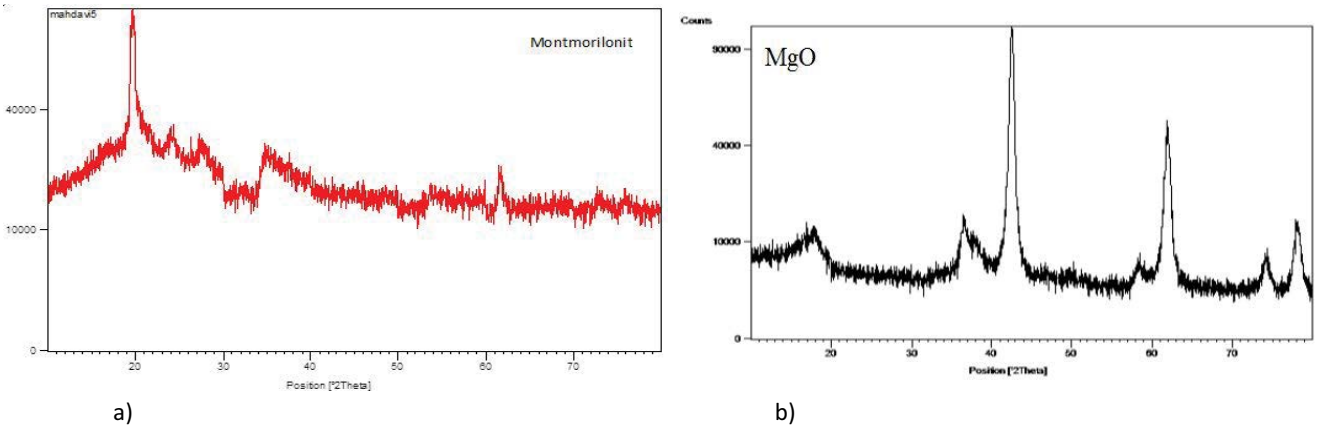

Fig. 2. XRD plot of Mont-NPs (a) and MgO-NPs (b).

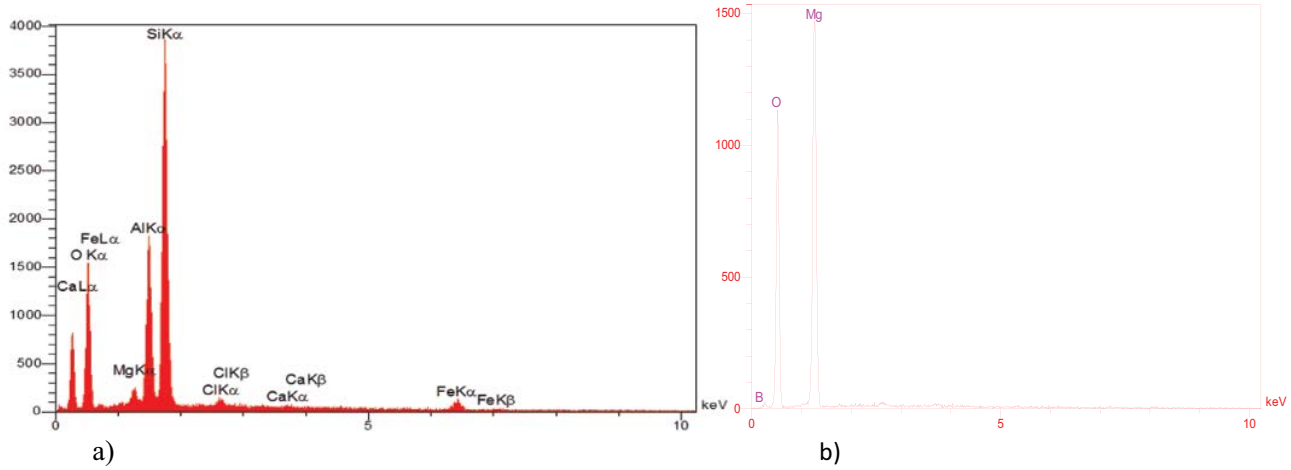

Fig. 3. EDX spectra of Mont-NPs (a) and MgO-NPs (b).

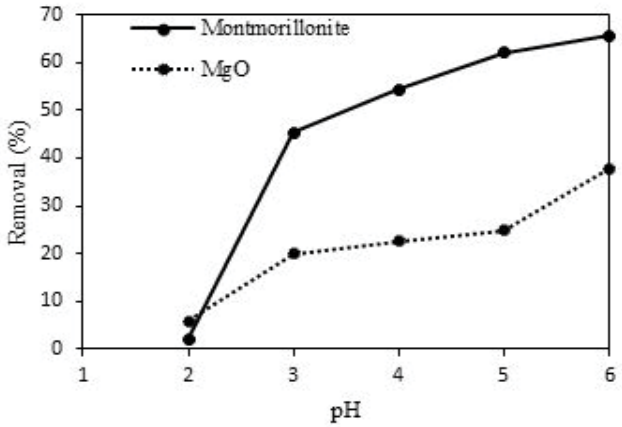

Fig. 4. Effect of pH on Co(II) removal by the adsorbents.

the adsorption process, highly depends on the solution's pH by montmorillonite adsorbent [27].

As shown in Fig. 4, any increase in the pH values of the solution mounted the heavy metal removal for both adsorbents. Line graphs for the adsorbents followed an upward trend, but the increased removal was more dramatic for Mont-NPs due to its dosage, nature of clay such as high surface area, high inter-layer space, and free intrinsic negative as well. Furthermore, the maximum removal occurred at pH 6.

Losing hydrogen ions in the active sites of the adsorbents at higher pH advances the adsorption of Co(II) ions. At low pH, hydrogen ions, which have a positive charge, are abundant on the adsorbent's surface. They had a competitive behavior with Co(II) ions which would lead to weak adsorption for both adsorbents. Notably, the precipitation mechanism of MgO-NPs as well as an increased pH value (from 5 to 6), would justify the 13% observed difference between the two latter points of the MgO-NPs figure.

3.3. *Effect of adsorbent dosage*

The impact of the adsorbent dosage on heavy metal uptake can be seen in Fig. 5. The adsorption rate for Mont-NPs steadily rose from 17.3% to 22.17%, when its dosage had changed from 1 to 5 g/L; likewise, for MgO-NPs, the

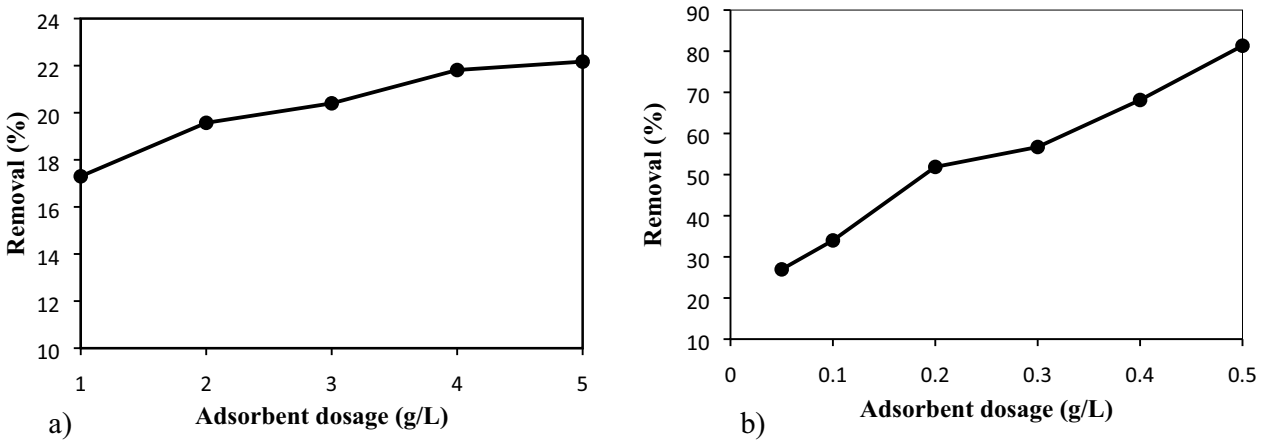

Fig. 5. Effect of adsorbent dosage Mont-NPs (a) and MgO-NPs (b).

removal percentage soared from 26.96% to 81.33% by increasing its dosage from 0.05 to 0.5 g/L. This figure illustrates a considerable difference between MgO-NPs and Mont-NPs, in Co(II) ions adsorption. It indicates the lower dosages of MgO-NPs have a higher strength for removing the same concentration of the pollutant. The high electrostatic charge of the Mont-NPs and its water molecules contiguity underlies forming bigger particles; hence, the active surface site for adsorption dwindles considerably. As seen, any increase in the adsorbent dosage does not have an apparent impact on the Co(II) ions removal. Therefore, the equilibrium attained for this adsorbent in 5 g/L as the line graph leveled off at 22%, roughly.

Higher dosages of adsorbents have more active sites for ions; this concept was more favorable for MgO-NPs adsorbents. As shown in Fig. 5 and supplementary charts, a higher dose removes more Co(II) ions from the solution. For a better understanding of the MgO-NPs dosage effect on Co(II) adsorption, more tests were carried out by rising dosages from 0.05 to 0.5 g/L, while the other experiment circumstances were the same; the results are available in supplementary figures.

3.4. Effect of temperature and thermodynamic discussion

Temperature tests revealed that temperature increments decided about a 3% difference between the minimum and the maximum amounts for Mont-NPs, mounting to 18.35% removal rate at 35°C. Meanwhile, the optimum temperature for MgO-NPs adsorbent was observed at 25°C. Negative $\Delta G°$ and $\Delta H°$ values for MgO-NPs signifies the spontaneous and exothermic nature of the reactions. The high negative $\Delta S°$ value also shows a downturn in the randomness of the adsorbed ions, which points to a fair adsorption process. Regarding the magnitude of $\Delta S°$ and $\Delta H°$, the reverse process of the adsorption needs high energy due to the firm covalent bond of Mg^{2+} with the solution anions.

Table 1 additionally gives information about the Mont-NPs thermodynamic parameters, representing the difference between the behavior of the two adsorbents. The table explains that the process of Co(II) ion removal by Mont-NPs adsorbent was endothermic; thus, a better condition for those reactions could be available in higher temperatures; additionally, there was a decline in the degree of freedom and randomness for the adsorbed particles [28]. Remarkably, MgO-NPs had higher entropy, showing that the adsorption process for these particles was far favorably performed than the Mont-NPs. Enthalpy magnitude may show the adsorption type [23]; thus, removal potency of MgO-NPs due to its higher values can be defined by adsorption and precipitation mechanisms, and the lower amount of enthalpy for Mont-NPs can be attributed to the lower adsorption rate. Accordingly, the electrostatic force was the main mechanism of the removal reactions [7].

A possible reason for positive enthalpy and Gibbs free energy could be the initial high concentration of Co^{2+} ions in confronting low adsorption capacity and the high dosages of Mont-NPs. Lower cobalt ion concentration in contact with Mont-NPs surfaces would have a better condition for adsorption into the active sites. As a result, less energy would take to provide a conducive placement for ions. Presumably, adsorption could happen to a greater extent at higher temperatures. The results of temperature impact and thermodynamic parameters are available in Fig. 6 and Table 1.

3.5. Effect of contact time and the kinetic modeling study

Fig. 7 depicts the effect of Co(II) ion contact and the adsorbents from 2 to 240 min. The removal value was 19.05% in 2 min after the contact with Mont-NPs, and it gradually dropped for the next 4 points of evaluation. At the same time, it seems that the reaction reaches equilibrium after 1 h, due to no significant change in the figures. For the MgO-NPs, the trend was vice versa, with a removal rate of about 24.41% (after 2 min). It was slightly increased where it reached to 26.21% in 60 min. After that, no considerable change was observed in the magnitude of the data.

The removal rate at the first points was fast (particularly for MgO-NPs). After 1 h, an equilibrium time was achieved for both adsorbents in Co(II) ion removal, with an initial Co(II) ion concentration of 70 mg/L. For MgO-NPs, with more contact time (the condition of shaking), cobalt ions were adsorbed by remained nanoparticles of the solution. As noted, any adsorbent has a specific capacity and active

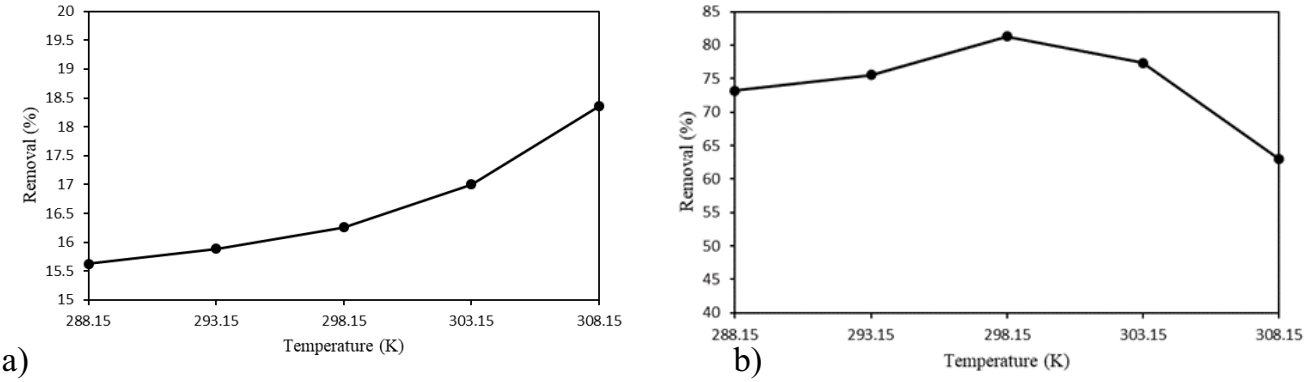

Fig. 6. Effect of temperature on adsorption of Co(II) ion onto Mont-NPs (a) and MgO-NPs (b).

Table 1
Thermodynamic parameter of adsorption (Co(II) concentration 70 mg/L)

Adsorbent	Thermodynamic parameters			
	T	$\Delta G°$	$\Delta S°$	$\Delta H°$
	(K)	(kJ/mol)	(J/mol K)	(kJ/mol)
Mont-NPs	288.15	4.11	–4.15	2.68
	293.15	4.06	–4.15	2.68
	298.15	4.06	–4.15	2.68
	303.15	3.99	–4.15	2.68
	308.15	3.82	–4.15	2.68
MgO-NPs	288.15	–7.92	–22.67	–13.97
	293.15	–8.68	–22.67	–13.97
	298.15	–9.35	–22.67	–13.97
	303.15	–8.76	–22.67	–13.97
	308.15	–7.26	–22.67	–13.97

sites, so the adsorption process gradually stagnates, and no conspicuous change will appear after reaching the equilibrium condition. On the other hand, as known, Mont-NPs have a high tendency for aggregation; after shaking, there was more chance for the adsorbed ions to be released into the solution, which increases the cobalt ion concentration.

Pseudo-first-order kinetic model only depends on the number of available metal ions in the solution; in contrast, the pseudo-second-order kinetic model is related to the number of free metal ions and the active surface sites [29]. The pseudo-first-order kinetic model was fitted with the MgO-NPs experimental data (R^2 = 0.99, k_1 = 0.018). The relevant result is available in Fig. 8, where a plot for log ($q_e - q_t$) vs. t (min) illustrates the kinetic data. Pseudo-second-order kinetic model fitted for both experimental adsorption data. The correlation coefficient values of both adsorbents were 0.99, which showed the perfect data fitting with this model. Table 2 demonstrates the parameters of the pseudo-second-order kinetic model for both adsorbents.

3.6. Adsorption isotherms

Langmuir model utilizes both physical and chemical adsorption descriptions, and it also describes the sorption on homogeneous sites of the adsorbent. It represents monolayer coverage at the high concentration on a finite identical spot of the adsorbent as well [30,31]. Freundlich model is an empirical equation, which also uses for heterogeneous surfaces of the adsorbents and multilayer sorption [32].

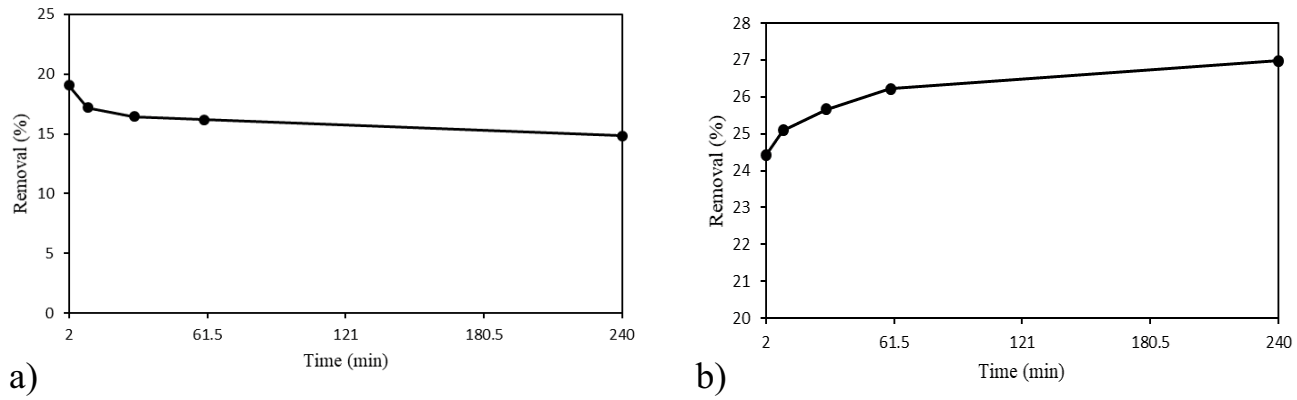

Fig. 7. Effect of contact time by Mont-NPs (a) and MgO-NPs (b) adsorbent.

MgO-NPs in contact with water molecules become hydroxylated, and $(OH)^-$ groups on the surface of the adsorbent continuously attack the Mg^{2+} ions. Some of these cationic ions dissolve in water to be Mg^{2+} ions, and some remain on the surface of the adsorbent, supplying nucleation sites for the generation of $Mg(OH)_2$ and (MgO) [33]. The high adsorption rate of MgO-NPs can be justified by adsorption of Co(II) ion on $Mg(OH)_2$ surfaces, generating after hydrolysis of MgO-NPs. Another contributing mechanism was precipitation of Co(II) ion into (MgO) form after contact with oxygen ion of the adsorbent. Meanwhile, MgO-NPs were hydrated to $Mg(OH)_2$, and the freely available hydroxyl groups at the surface of $Mg(OH)_2$ would provide bonding opportunities to form $Co(OH)_2$ and $Co(OH)^+$ providing further removal rate for this adsorbent. Removal of Co(II) ion onto Mont-NPs occurred by ion exchange and formation of complexes on silicate and alumina groups at edges of the Mont-NPs [34].

For both adsorbents, any gain in the initial concentration of cobalt ion had a positive impact on adsorption capacity. Experimental data for both adsorbents had a good affinity with the two isotherm models. As the coefficient of determinations (R^2) for both isotherms were near to unity, it can be described that the adsorption procedure for both adsorbents was a monolayer and multilayer phenomenon. The calculated (n) parameter in Freundlich's equation (3.108 and 4.97) ranged from 2 to 10, implying a favorable adsorption process. The adsorption capacities of cobalt ion (70 mg/L) by Mont-NPs and MgO-NPs adsorbents were 2.53 and 440 mg/g, respectively. Calculated q_{max} in Langmuir isotherm was in accordance with experimental figures, presented in Fig. 9. There is another dimensionless parameter, separation factor (R_L), which verifies the adsorption process and feasibility of Langmuir isotherm [35] that is explained below:

$$R_L = \frac{1}{1 + bC_0} \tag{10}$$

where b is the Langmuir constant (L/mg), C_0 is the final equilibrium concentration or the highest initial

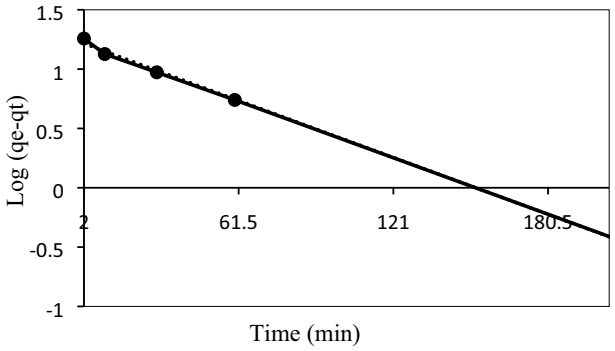

Fig. 8. Pseudo-first-order kinetic model plot for MgO-NPs adsorbent.

Table 2
Constants of pseudo-second-order kinetic model (Co(II) concentration = 70 mg/L)

Adsorbent	q_e	R^2	k_2
Mont-NPs	10.33	0.99	–0.04
MgO-NPs	188.67	0.99	4.92×10^{-3}

Table 3
Langmuir isotherm constants

Adsorbent	K_L	R^2	q_{max}
Mont-NPs	0.08	0.962	2.86
MgO-NPs	0.262	0.993	454.54

Table 4
Freundlich isotherm constants

Adsorbent	K_f	R^2	n
Mont-NPs	0.649	0.965	3.108
MgO-NPs	201.74	0.982	4.97

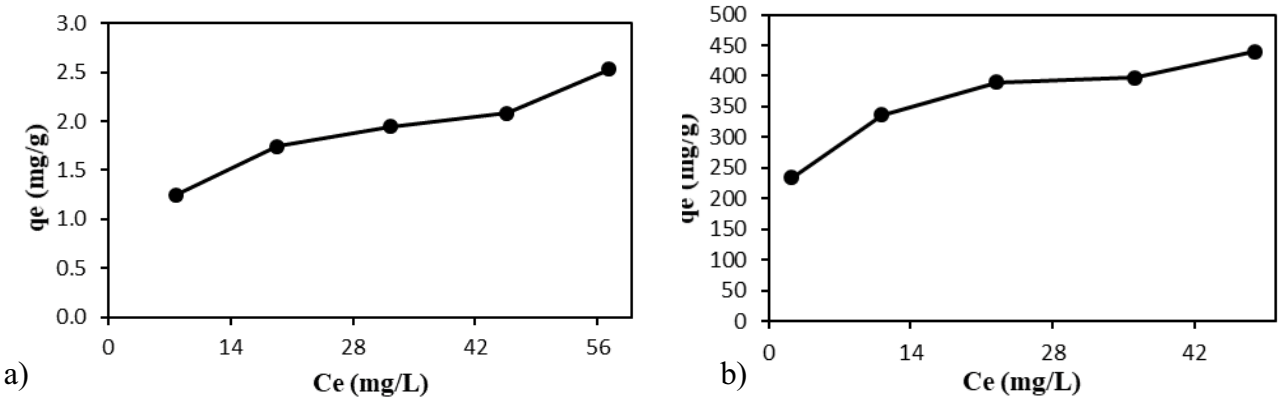

Fig. 9. Adsorption isotherm of Mont-NPs (a) and MgO-NPs (b).

Table 5
Adsorption capacity for Co(II) removal in different studies

References	Capacity (mg/g)	Adsorbent
[23]	480	POP600 (activated carbon)
[32]	21.93	Resin (Lewatit MonoPlus SP 112)
[28]	82.64	Modified *Ficus carica* leaves
[31]	16.86 (pH 9.0)	Natural bentonite
[36]	70.04	Polypyrrole particles
[29]	29.48	Teak (*Tectona grandis*) leaves powder
[37]	6.3	Black carrot residues
[38]	13.73	Chemically modified marine algae
This study	440	MgO-NPs
This study	2.53	Mont-NPs

concentration of the metal ion solution. The calculated R_L for the Mont-NPs and MgO-NPs in optimum condition were 0.179 and 0.073, respectively. As these values were less than 1, it shows excellent adsorption for MgO-NPs, mainly [35].

The Langmuir and Freundlich calculated parameters are depicted in Tables 3 and 4; also, different adsorbent capacities in the literature are compared, outlined in Table 5.

3.7. Desorption studies

Results showed that the desorbed Co(II) ion concentrations in the solution which contained the Mont-NPs and MgO-NPs were trace and 0.33 mg/L, respectively. This can be counted as an infinitesimal portion in comparison to the equilibrium concentration. One would conclude that the adsorbents were capable of retaining the adsorbed ions in the presence of chloride ions by the implemented method for desorption.

4. Conclusion

In summary, the SEM technique showed the Mont-NPs and MgO-NPs diameters were in the range of nano-size. pH, contact time, temperature, and adsorbents dosage had a significant effect on the adsorption of Co(II) ion by the adsorbents. Freundlich and Langmuir isotherm models fitted to the equilibrium data of the adsorbents. Equilibrium data of the adsorbents were well-defined by the pseudo-second-order kinetic model (for both of the absorbents) and the pseudo-first-order model (only for MgO-NPs). The thermodynamic study revealed that the process of the adsorption for MgO-NPs and Mont-NPs were exothermic and endothermic, with a decline in the freedom degree for both adsorbents. Maximum adsorption capacities for the initial Co(II) ion (70 mg/L concentration) were 2.53 and 440 (mg/g) for Mont-NPs and MgO-NPs, respectively. MgO-NPs and Mont-NPs had a remarkable ability for Co(II) adsorption. Still, MgO-NPs had a far greater potential for Co(II) ion removal because of its nanostructure, more adsorption surface, and the precipitation process; compared with the Mont-NPs.

References

[1] S. Khan, Q. Cao, Y.M. Zheng, Y.Z. Huang, Y.G. Zhu, Health risks of heavy metals in contaminated soils and food crops irrigated with wastewater in Beijing, China, Environ. Pollut., 152 (2008) 686–692.
[2] S. Joshi, H. Singh, S. Sharma, P. Barman, A. Saini, G. Verma, Synthesis and characterization of graphene oxide-bovine serum albumin conjugate membrane for adsorptive removal of cobalt(II) from water, Int. J. Environ. Sci. Technol., (2021) 1–14, doi: 10.1007/s13762-020-03050-y.
[3] D. Joksimovic, I. Tomic, A.R. Stankovic, M. Jovic, S. Stankovic, Trace metal concentrations in Mediterranean blue mussel and surface sediments and evaluation of the mussels quality and possible risks of high human consumption, Food Chem., 127 (2011) 632–637.
[4] H.N. Bhatti, R. Khadim, M.A. Hanif, Biosorption of Pb(II) and Co(II) on red rose waste biomass, Iran. J. Chem. Chem. Eng., 30 (2011) 81–87.
[5] V.K. Gupta, A. Mittal, L. Krishnan, J. Mittal, Adsorption treatment and recovery of the hazardous dye, Brilliant Blue FCF, over bottom ash and de-oiled soya, J. Colloid Interface Sci., 293 (2006) 16–26.
[6] S. Mahdavi, M. Jalali, A. Afkhami, Heavy metals removal from aqueous solutions using TiO_2, MgO, and Al_2O_3 nanoparticles, Chem. Eng. Commun., 200 (2013) 448–470.
[7] S. Seif, S. Marofi, S. Mahdavi, Removal of Cr^{3+} ion from aqueous solutions using MgO and montmorillonite nanoparticles, Environ. Earth Sci., 78 (2019) 1–10.
[8] S. Mahdavi, P. Molodi, M. Zarabi, Utilization of bare MgO, CeO_2, and ZnO nanoparticles for nitrate removal from aqueous solution, Environ. Prog. Sustainable Energy, 37 (2018) 1908–1917.
[9] S. Mahdavi, Z. Tarhani, A.M. Sayyahzadeh, E.N. Peikam, Effect of nano-MgO, biochar and humic acid on boron stabilization in soil in bath and leaching columns, Soil Sediment Contam.: Int. J., 29 (2020) 595–612.
[10] S. Mahdavi, M. Zarabi, Functionalized MgO, CeO_2 and ZnO nanoparticles with humic acid for the study of nitrate adsorption efficiency from water, Res. Chem. Intermed., 44 (2018) 5043–5062.
[11] M.S. Gasser, GH.A. Morad, H.F. Aly, Batch kinetics and thermodynamics of chromium ions removal from waste solutions using synthetic adsorbents, J. Hazard. Mater., 142 (2007) 118–129.
[12] C.T. Campbell, D.E. Starr, Metal adsorption and adhesion energies on MgO(100), J. Am. Chem. Soc., 124 (2002) 9212–9218.
[13] T.J. Pinnavaia, Intercalated clay catalysts, Science, 220 (1983) 365–371.
[14] M.F. Brigatti, E. Galán, B.K.G. Theng, Chapter 2 – Structure and Mineralogy of Clay Minerals, F. Bergaya, G. Lagaly, Eds., Developments in Clay Science, Vol. 5A, Elsevier Press, Amsterdam, 2013, pp. 21–68.
[15] F. Barraqué, M.L. Montes, M.A. Fernández, R. Candal, R.M. Torres Sánchez, J.L. Marco-Brown, Arsenate removal from aqueous solution by montmorillonite and organo-montmorillonite magnetic materials, Environ. Res., 192 (2021) 110247, doi: 10.1016/j.envres.2020.110247.

[16] S.R. Liu, M. Chen, X.Q. Cao, G. Li, D. Zhang, M.Z. Li, N. Meng, J.J. Yin, B.Q. Yan, Chromium(VI) removal from water using cetylpyridinium chloride (CPC)-modified montmorillonite, Sep. Purif. Technol., 241 (2020) 116732, doi: 10.1016/j.seppur.2020.116732.
[17] H.P. Klug, L.E. Alexander, X-ray Diffraction Procedures: For Polycrystalline and Amorphous Materials, 2nd ed., Wiley, New York, 1974, p. 618.
[18] M.M. Abou-Mesalam, Sorption kinetics of copper, zinc, cadmium and nickel ions on synthesized silico-antimonate ion exchanger, Colloids Surf., A, 225 (2003) 85–94.
[19] S. Lagergren, Zur Theorie der sogenannten Adsorption gelöster Stoffe, Kungliga Svenska Vetenskapsakademiens, Handler, 24 (1898) 1–39.
[20] Y.S. Ho, G. McKay, Pseudo-second order model for sorption processes, Process Biochem., 34 (1999) 451–465.
[21] K.-Y. Shin, J.-Y. Hong, J.S. Jang, Heavy metal ion adsorption behavior in nitrogen-doped magnetic carbon nanoparticles: isotherms and kinetic study, J. Hazard. Mater., 190 (2011) 36–44.
[22] K.H. Tan, Principles of Soil Chemistry, CRC Press Inc., Boca Raton, FL, USA, 2010.
[23] G.Z. Kyzas, E.A. Deliyanni, K.A. Matis, Activated carbons produced by pyrolysis of waste potato peels: cobalt ions removal by adsorption, Colloids Surf., A, 490 (2016) 74–83.
[24] A.K. Helmy, E.A. Ferreiro, S.G. De Bussetti, Cation exchange capacity and condition of zero charge of hydroxy-A1 montmorillonite, Clays Clay Miner., 42 (1994) 444–450.
[25] C. Bulin, Y.H. Zhang, B. Li, B.W. Zhang, Removal performance of aqueous Co(II) by magnetic graphene oxide and adsorption mechanism, J. Phys. Chem. Solids, 144 (2020) 109483, doi: 10.1016/j.jpcs.2020.109483.
[26] D. Gogoi, T. Kumar, A.G. Shanmugamani, S.V.S. Rao, P.K. Sinha, Studies on removal of cobalt from an alkaline waste using synthetic calcium hydroxyapatite, J. Radioanal. Nucl. Chem., 298 (2013) 337–344.
[27] K.G. Bhattacharyya, S.S. Gupta, Adsorption of a few heavy metals on natural and modified kaolinite and montmorillonite: a review, Adv. Colloid Interface Sci., 140 (2008) 114–131.
[28] R. Dabbagh, Z. Ashtiani Moghaddam, H. Ghafourian, Removal of cobalt(II) ion from water by adsorption using intact and modified *Ficus carica* leaves as low-cost natural sorbent, Desal. Water Treat., 57 (2015) 19890–19902.
[29] S. Vilvanathan, S. Shanthakumar, Removal of Ni(II) and Co(II) ions from aqueous solution using teak (*Tectona grandis*) leaves powder: adsorption kinetics, equilibrium and thermodynamics study, Desal. Water Treat., 57 (2014) 3995–4007.
[30] M. Deravanesiyan, M. Beheshti, A. Malekpour, Alumina nanoparticles immobilization onto the NaX zeolite and the removal of Cr(III) and Co(II) ions from aqueous solutions, J. Ind. Eng. Chem., 21 (2015) 580–586.
[31] Ş. Kubilay, R. Gürkan, A. Savran, T. Şahan, Removal of Cu(II), Zn(II) and Co(II) ions from aqueous solutions by adsorption onto natural bentonite, Adsorption, 13 (2007) 41–51.
[32] Y. Aşçı, Ş. Kaya, Removal of cobalt ions from water by ion-exchange method, Desal. Water Treat., 52 (2014) 267–273.
[33] S. Xu, Z. Zhong, W.Z. Liu, H. Deng, Z. Lin, Removal of Sb(III) from wastewater by magnesium oxide and the related mechanisms, Environ. Res., 186 (2020) 109489, doi: 10.1016/j.envres.2020.109489.
[34] M. Tokarčíková, J. Seidlerová, O. Motyka, O. Životský, K. Drobíková, R. Gabor, Experimental verification of regenerable magnetically modified montmorillonite and its application for heavy metals removal from metallurgical waste leachates, J. Water Process Eng., 39 (2021) 101691, doi: 10.1016/j.jwpe.2020.101691
[35] P.N. Dave, N. Subrahmanyam, S. Sharma, Kinetics and thermodynamics of copper ions removal from aqueous solutions by use of activated charcoal, Indian J. Chem. Technol., 16 (2009) 234–239.
[36] L. Seid, D. Chouder, N. Maouche, I. Bakas, N. Barka, Removal of Cd(II) and Co(II) ions from aqueous solutions by polypyrrole particles: kinetics, equilibrium and thermodynamics, J. Taiwan Inst. Chem. Eng., 45 (2014) 2969–2974.
[37] F. Güzel, H. Yakut, G. Topal, Determination of kinetic and equilibrium parameters of the batch adsorption of Mn(II), Co(II), Ni(II) and Cu(II) from aqueous solution by black carrot (*Daucus carota* L.) residues, J. Hazard. Mater., 153 (2008) 1275–1287.
[38] R. Foroutan, H. Esmaeili, M. Abbasi, M, Rezakazemi, M. Mesbah, Adsorption behavior of Cu(II) and Co(II) using chemically modified marine algae, Environ. Technol., 39 (2017) 2792–2800.

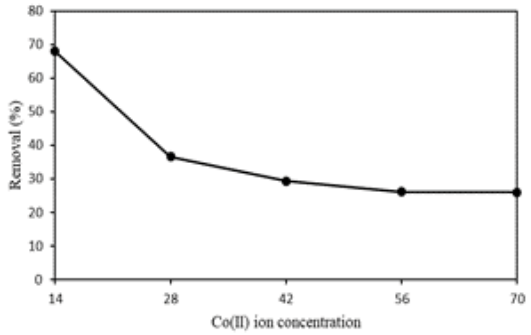

MgO-NPs dosage (0.05 g/L)

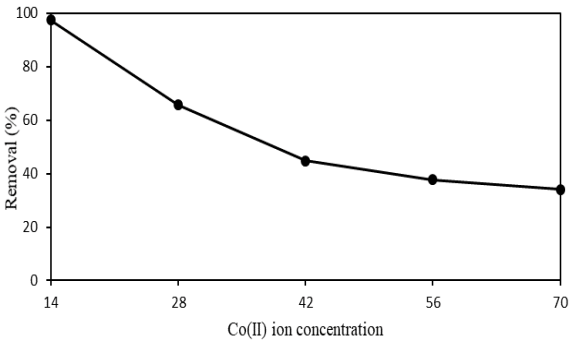

MgO-NPs dosage (0.1 g/L)

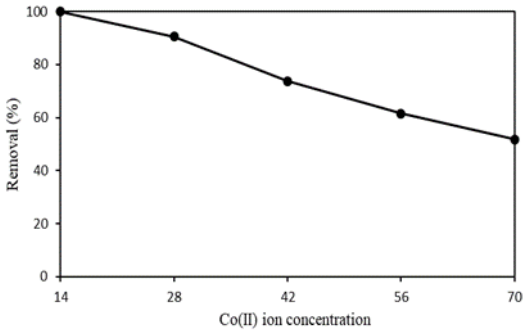

MgO-NPs dosage (0.2 g/L)

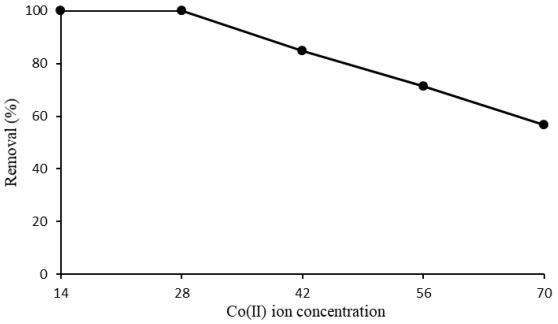

MgO-NPs dosage (0.3 g/L)

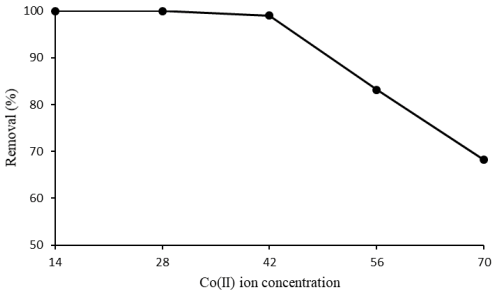

MgO-NPs dosage (0.4 g/L)

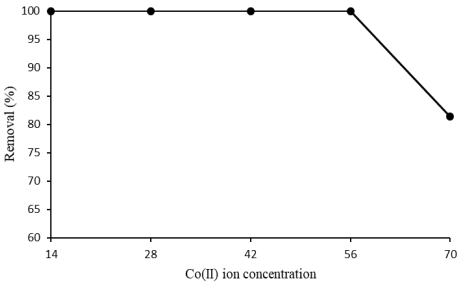

MgO-NPs dosage (0.5 g/L)